scientific reports

Check for updates

OPEN

A flow cytometry method for quantitative measurement and molecular investigation of the adhesion of bacteria to yeast cells

Marion Schiavone[1,2,4], Adilya Dagkesamanskaya[1,4], Pierre-Gilles Vieu[1], Maëlle Duperray[1], Valérie Duplan-Eche[3] & Jean Marie François[1]✉

The study of microorganism interactions is important for understanding the organization and functioning of microbial consortia. Additionally, the interaction between yeast and bacteria is of interest in the field of health and nutrition area for the development of probiotics. To investigate these microbial interactions at the cellular and molecular levels, a simple, reliable, and quantitative method is proposed. We demonstrated that flow cytometry enables the measurement of interactions at a single-cell level by detecting and counting yeast cells with bound fluorescent bacteria. Imaging flow cytometry revealed that the number of bacteria attached to yeast followed a Gaussian distribution whose maximum reached 14 bacterial cells using a clinical *Escherichia coli* strain E22 and the laboratory yeast strain BY4741. We found that the dynamics of adhesion resemble a Langmuir adsorption model, albeit it is a rapid and almost irreversible process. This adhesion is dependent on the mannose-specific type 1 fimbriae, as *E. coli* mutants lacking these appendages no longer adhere to yeast. However, this type 1 fimbriae-dependent adhesion could involve additional yeast cell wall factors, since the interaction between bacteria and yeast mutants with altered mannan content remained comparable to that of wild-type yeast. In summary, flow cytometry is an appropriate method for studying bacteria-yeast adhesion, as well as for the high-throughput screening of candidate molecules likely to promote or counteract this interaction.

Keywords Yeast, Bacteria, Adhesion, Cell wall, Fimbriae, Flow cytometry

A number of studies have highlighted the beneficial effects of adding whole yeasts or yeast cell walls to animal feed in terms of health and growth performance[1–4], leading to the development of probiotics and paraprobiotics process as mean to provide protective effects to the ingesting host[5]. These protective effects provided by probiotic (viable organisms) or paraprobiotic (non-viable micro-organisms or fractions thereof) according to FAO definition (FAO/WHO, 2001; https://www.fao.org/3/a0512e/a0512e.pdf) are suggested to be mostly due to components of the cell wall products that act as anti-adhesive agents preventing attachment of bacteria to the surface of intestinal mucosal[6,7]. This suggestion is based on the finding that bacterial adhesion to intestinal mucosa is achieved by glycoproteins abundantly present in the membrane of these host cells carrying N-linked mannose structures that bind to bacterial mannose-specific type 1 fimbriae[8–10]. As yeast cell wall are enriched with proteins highly decorated with mannosyl sugars that represents about 40% of the cell wall mass[11–13], these components can act as antagonist to mannosyl sugars of the host glycoproteins[14,15]. However, bacteria adhesion to intestinal cells can also occur by other means, such as by afimbrial autotransporter (AT) adhesins that are present among Enterobacteriaceae family of the *Escherichia* genus[16], or the outer membrane protein Tia encoded by the locus *tia* and produced by some enterotoxigenic *E. coli* (ETEC)[17]. In addition, other yet unknown factors

[1]Toulouse Biotechnology Institute (TBI), UMR INSA-CNRS 5504 & INRA 792, 135 Avenue de Rangeuil, 31077 Toulouse, France. [2]Lallemand SAS, 19, Rue Des Briquetiers, 31702 Blagnac, France. [3]Institut Toulousain Des Maladies Infectieuses Et Inflammatoires (Infinity), CNRS U5051, INSERM U1291, University Toulouse III, 31000 Toulouse, France. [4]These authors contributed equally: Marion Schiavone and Adilya Dagkesamanskya. ✉email: fran_jm@insa-toulouse.fr

in addition to mannans could have a role in interaction of bacteria to yeast cells as suggested by work of Ganner et al.[18,19] and Tiago et al.[20] showing no correlation between cell wall mannan content and bacterial adhesion. Overall, the mechanism of bacteria-yeast interaction and the nature of the molecular components involved in this interaction are still largely unknown.

To study the adhesion of bacteria to yeast cells and to characterize the effects of probiotics and paraprobiotics[21] to prevent bacteria attachment to intestinal cells, a simple and reliable method is essential. This method must be quantitative, capable of being used to high throughput screening of compounds likely to affect this adhesion, and above all, this method must be able of measuring the adhesion of bacteria with yeast on a single cell level in order to overcome the problems of aggregation that can happen with both bacterial and yeast cells. This analysis on a single cell scale should also make it possible to understand the molecular mechanisms of this interaction. To date, the different methods that have been set up to measure bacteria-yeast interaction do not fulfill these requirements. This is notably the case for the agglutination method originally developed by Mirelman et al.[22]. In this method, bacterial cells are incubated with yeast cells for a certain period of time, which is followed by visual examination under the microscope. Results obtained can be highly subjective and operator dependent, and bacteria trapped into yeast aggregates are hardly distinct from those that adhere to yeast cells. Also, the sedimentation method which is based on counting bacterial cells that did not sediment with yeast cells during co-incubation is poorly reliable because of many false positive data due to bacteria that are just entrapped in cell aggregates[20,23]. Likewise for the filtration method, which enables a direct counting of bacteria bound to yeast cells but cannot distinguish between true binding and entrapment. A microplate assay initially developed by Becker et al.[24] and optimized by Ganner et al.[19] used the optical density measurement as a growth parameter for bacteria bound to yeast cell wall products retained in microtiter plate wells. The principle is based on an inverse relationship between initial cell densities and the resumption of growth: the higher the number of adherent cells, the shorter the time taken for bacterial growth to resume, likely because of the effect of local concentration of cells. This method, albeit simple to set up and more reliable than those previously described, presents same artifacts of false positive interaction as those previous ones. Other methods like direct visualization of interaction using scanning electronic microscopy[5,14,23] or parallel-plate flow chamber that could get around some of the limitations described above were set up[25], but they have also serious restrictions including the duration of sample preparation, experimental set-up and measurement. Therefore, these methods are not suitable as a screening tool for investigating effectors and parameters involved in the interaction.

In this report, we show that the conventional and image flow cytometry is an appropriate tool to directly and quantitatively investigate the adhesion of bacteria to yeast cells. After establishing the standard procedure for accurate and quantitative measurement of adhesion of bacteria to yeast cells, we validated our method by testing the *E. coli* mutants lacking type 1 fimbriae (or type 1 pili) as well as yeast mutants with altered content of the mannoproteins in the cell wall.

Results

Flow cytometry as a reliable method for investigate bacteria-yeast adhesion

A mix of bacteria and yeast incubated for 1 h at 37 °C in PBS buffer placed under the microscope revealed a physical contact between these two microorganisms, whether this image was taken in bright field or imaged after excitation at 490 nm to collect green fluorescence emitted by the bacterial cells expressing the green fluorescent Dendra2 protein (Fig. 1A). While some bacteria appeared to adhere to yeast cell, others were probably trapped in the aggregates formed by several yeast cells. Therefore, to be quantitative and free from artifacts, a flow cytometry-based method capable of quantifying the cell-to-cell interaction was developed. The two microorganisms independently analyzed appear in two distinct populations based on morphology and fluorescence characteristics. Indeed, the size and morphology of bacteria and yeast are very different, which enables to distinguish them on forward scatter (FSC) versus side scatter (SSC)-area using classical gating strategies (Fig. 1B,C upper panel). Analysis of yeast cells alone led to a peak of low fluorescence intensity with median values of 200–300 A.U., corresponding to the natural fluorescence of yeast cells (autofluorescence), while the recording of *E. coli* cells expressing the green fluorescent protein Dendra2 led to a single peak of higher fluorescence intensity with median values in the range of 300,000–400,000 A.U. (Fig. 1B,C lower panel). After incubation of a mix of yeast cells (approx. 10^8 cells) with green fluorescent *E. coli* cells (approx. 10^9 cells) for 90 min at 37 °C followed by a quick wash with PBS buffer, the suspension was analyzed by flow cytometry. A high fluorescence intensity was recorded at the gating events of yeast population, indicating the presence of bacterial cells attached to yeast cells. Accordingly, two distinct peaks were resolved within the yeast population; a first one that counted for the autofluorescence of yeast cells and a second peak that corresponded to bacteria attached to yeast singlets (Fig. 1D). However, to quantify these interactions, only single yeast cells (singlets) with similar cell size and granularity based on the FSC-A (area) and FSC-H (height) plot had to be retained (Fig. S1). The cell counts of the "fluorescent" yeast population was thus taken to calculate an adhesion index (A_i) that corresponded to the number of singlets yeast that have at least one bacterium bound to the total number of yeast singlets.

To ensure that A_i reflected true binding of bacteria to yeast cells, we performed several washes before measuring fluorescence by flow cytometry. A_i decreased by less than 10% after two successive washes and then remained stable over the next washes (see Fig. S2 in suppl. data). In addition, we investigated the effect of incubation time on the yeast-bacteria interaction and found that A_i value plateaued already after 10 min of co-incubation (see Fig. S2) and the value did not change with longer incubation times. Using imaging flow cytometry, the bacteria-to-yeast interaction was clearly visualized (Fig. 2A), allowing the quantification of the number of bacteria bound per yeast cell. This number of bound bacteria followed a Gaussian distribution, with a median value of 6 bacteria and a maximum of 14 (Fig. 2B), when the co-incubation was carried out with large excess of bacteria ($> 5 \times 10^9$) over yeast cells (10^8), giving rise to $A_i > 80\%$. When the number of bacteria was in the range of that of yeast cell

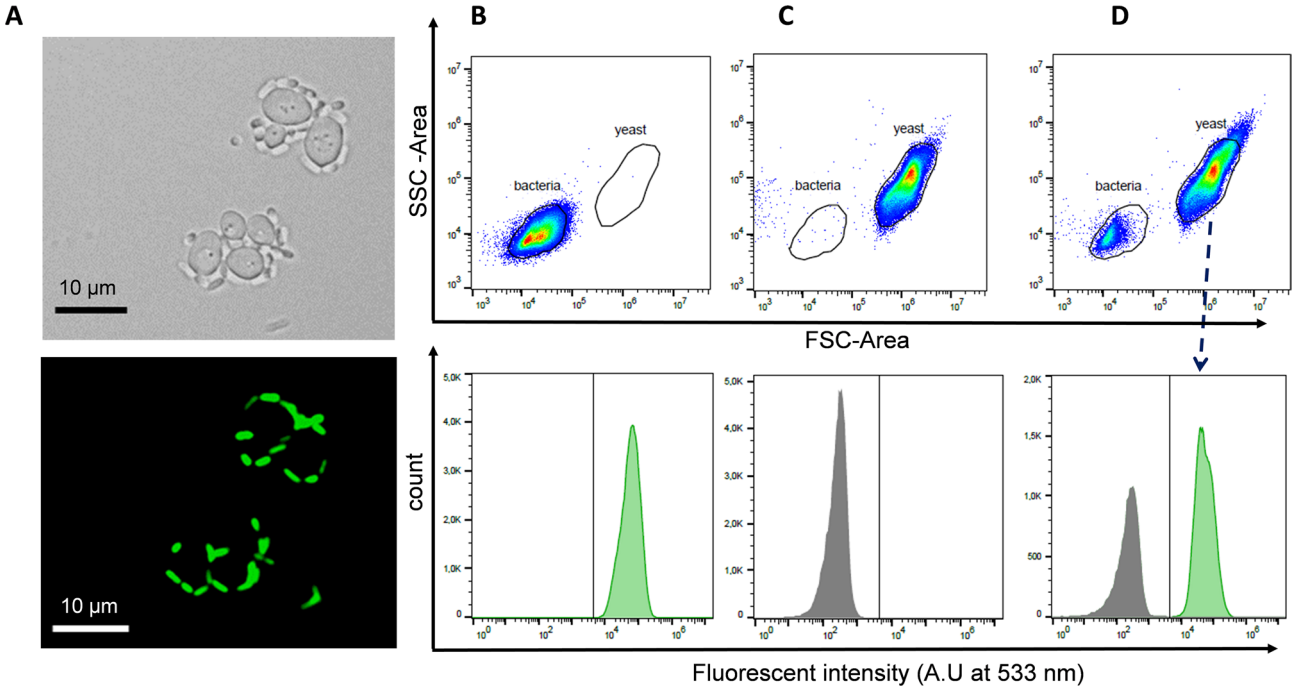

Figure 1. Flow cytometry measurements of bacteria—yeast adhesion. (**A**) Microscopy bright field and fluorescence images of incubation mixture of the *E. coli* E22 (10^9 cells/ml) expressing the green fluorescent protein Dendra2 with 10^8 BY4741 yeast cells/ml in PBS buffer. (**B**, **C**) Representative flow cytometry dot plots SSC-Area vs FSC-Area and corresponding fluorescence intensity histograms of *E. coli* E22 cells expressing the green fluorescent protein Dendra-2 (**B**) and *S. cerevisiae* BY4741 strain (**C**). In (**D**) is shown the flow cytometry dot plot SSC-Area vs FSC-Area of the mix yeast and bacteria and fluorescence intensity histogram of the yeast population (as indicated by the arrow).

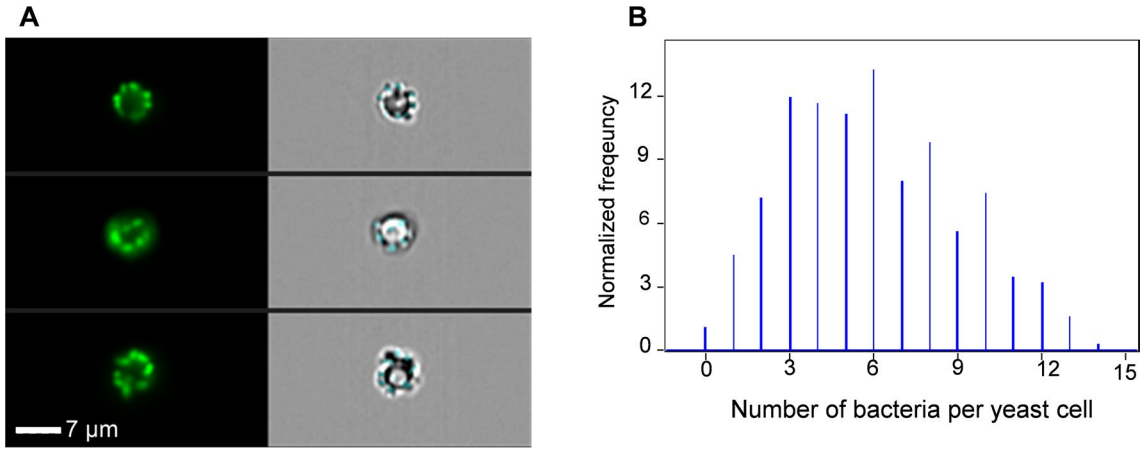

Figure 2. Imaging flow cytometry of yeast—bacteria interaction. (**A**) Image analysis of representative samples of bacteria retained to yeast cells as acquired on the ImageStreamX Mark II. (**B**) The number of bacteria attached per yeast cell using a ratio bacteria: yeast of 50 (5×10^9: 10^8 yeast cells) was quantified on about 1000 of single yeast cells.

(10^8 and $A_i \sim 10\%$), this value dropped to maximum of 5 bacteria per yeast cell with the median at 1 bacterium (data not shown).

To illustrate how the aggregation state of yeast, can lead to difference in percentage of singlets and inaccurate conclusions on bacterial adhesion, we used *gas1Δ* mutant, known to form strong cell–cell aggregates representing > 50% of the total population[26]. Assuming same amount of yeast cells based of OD_{600nm}, we found that the A_i of *E. coli* E22 strain with *gas1Δ* mutant was 3-times higher than with isogenic wild type (BY4741) cells. However, after sonication of the *gas1Δ* culture to destroy as much as possible the aggregates, and by this way increase the number of single yeast cells in the mixture, the A_i value became comparable to that of the wild type (Fig. S3 in suppl Data).

Dynamic aspects of bacteria -yeast adhesion and influence of environmental parameters

The flow cytometry-based method allowed to determine the dynamic of adhesion of bacteria to yeast by measuring A_i as a function of the number of bacteria that was co-incubated with a fixed number of yeast cells. As shown in Fig. 3, the plot obtained for two different bacteria strains, namely the laboratory *E. coli* K12 BW25113 and the clinical isolate *E. coli* E22 followed a hyperbolic curve that resembled a Langmuir adsorption model (inset a of Fig. 3). By plotting the inverse of A_i versus the inverse of bacterial cells concentration, a regression line was drawn from which an adhesion constant α that corresponded to the slope of these lines, could be calculated according to Eq. (3) described in Materials & Methods. This α value was 2.0-fold lower for clinical strain E22 than for laboratory strain BW25113 (1.22×10^{-6} cells^{-1} ml for E22 and 2.55×10^{-6} cell^{-1} ml for BW25113), indicating that E22 strain exhibited an apparent affinity to yeast higher than that of BW25113.

As emphasized elsewhere[27], it is not because the adhesion displays a Langmuir-like curve that this phenomenon agrees with a Langmuir adsorption isotherm, for which adsorption/desorption must be a reversible process. To know whether the adhesion of bacteria cells to yeast cells is dynamically reversible, we performed a competition between fluorescent and non-fluorescent bacteria. After the *E. coli* cells were co-incubated for 90 min with yeast cells, the mix was challenged with a tenfold excess of non-fluorescent *E. coli* cells and further incubated for 90 min before fluorescence measurement. Results of this experiment showed that the percentage of adhesion only decreased by 10% (Fig. 4). Same results were obtained even when the pre-incubation of fluorescent bacteria with yeast cells was carried out for shorter time (*ie* 10 min, data not shown). These results indicate that the adhesion of bacteria is fast, almost irreversible and hence may involve strong linkages between the two cells. Additionally, we found that pH, temperature and ionic strength had no significant effect on the adhesion of this *E. coli* E22 strain on the BY4741 yeast strain (see Fig. S4 in suppl. data).

Type 1 fimbriae are essential for adhesion of bacteria to yeast cells

To test the sensitivity and reliability of our method, we measured adhesion of various *E. coli* strains from laboratory and clinical collections to the laboratory yeast BY4741. We compared the adhesion index between all bacteria tested using the same number of bacterial cells (~ 10^9 cells) that were co-incubated with a fixed amount of BY4741 strain (10^8 cells), followed by two quick washing. Results in Fig. 5 showed that the clinical isolate *E. coli* E22 strain presented the highest adhesion index ($A_i \sim 93\%$) followed by another clinical isolate SP15 ($A_i \sim 82\%$) and then by the two laboratory K12-derivative strains BW25113 and DH5α, whose A_i was 25% lower than that of E22 strain (at $P < 0.001$). In contrast, BL21 and ccdB strains that belong to *E. coli* B. group as well as the clinical isolate M1/5 exhibited very poor adhesion ($A_i < 5\%$). This study highlighted the occurrence of at least three categories of bacteria distinguished by their adhesion capacity to yeast cells, namely high adherence as exemplified for E22 and SP15; moderate adherence for DH5α and BW25113 and weak to nil adherence for BL21, ccdB and M1/5 (high adherence was significantly distinct from moderate at $p < 0.05$ and moderate from weak at $p < 0.01$).

The absence of interaction of *E. coli* BL21 with yeast led us to question the role of type 1 fimbriae in this interaction, given that BL21 is deficient in the production of these extracellular structures[28,29]. This potential role is further supported by previous data showing that interaction to yeast cells was impaired in *E. coli* mutants defective in type 1 fimbriae[30–32]. To confirm with our method that these structures are implicated in adhesion of bacteria to yeast cells, *E. coli* BW251123 defective in *fimA*, encoding the rod-forming major subunit of type I

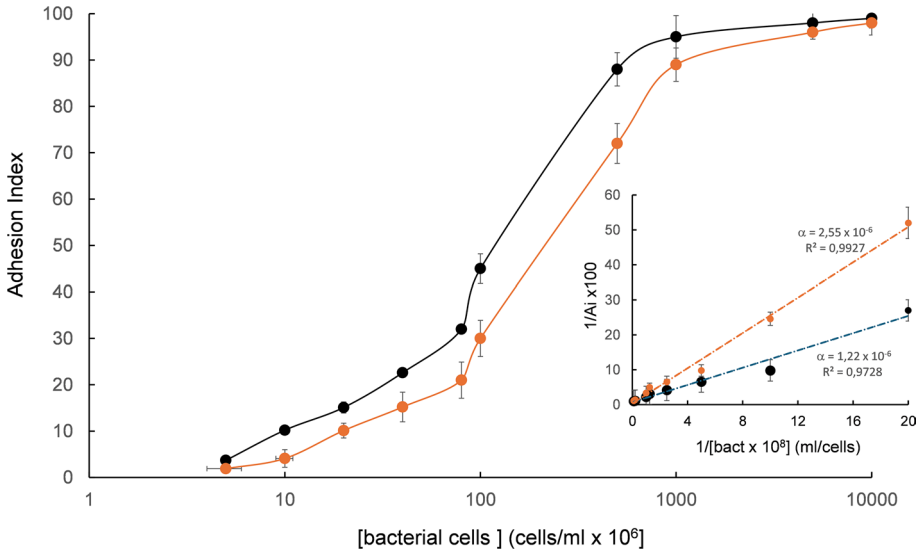

Figure 3. Adhesion of bacteria to yeast as a function of the concentration of bacteria. Dose-dependency of *E. coli* E22 (blue) or BW25113 (brown) cells concentration on adhesion to a fixed amount (10^8 cells/ml) BY4741 cells from three independent experiments carried out in PBS at pH 7 and 37 °C. Insert shows the plot $1/A_i$ vs 1/bact that enables to estimate the value α for these two bacteria interacting with.

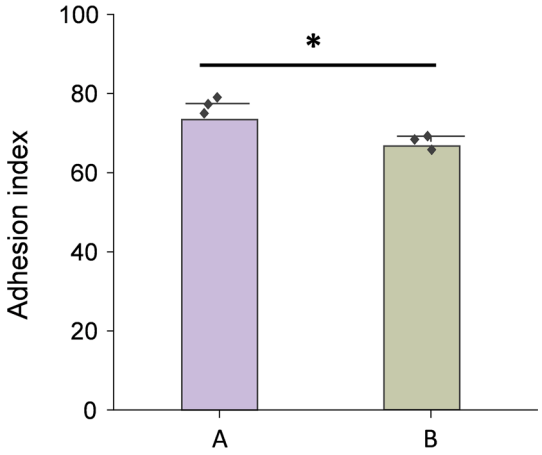

Figure 4. The adhesion of *E. coli* to yeast is an almost irreversible process. Adhesion index of bacteria-yeast before (**A**) and after the addition of an excess of non-fluorescent *E. coli* (**B**). Co-incubation of 10^8 BY4741 yeast cells and 5×10^9 *E. coli* E22 cells/ml expressing fluorescent Dendra2 protein was carried out at 37 °C for 90 min, followed by two washing steps. Then, the mix was split, and part was further washed with 5×10^{10} cells/ml of non-fluorescent E22 cells during 30 min prior to record fluorescence. *$p<0.05$.

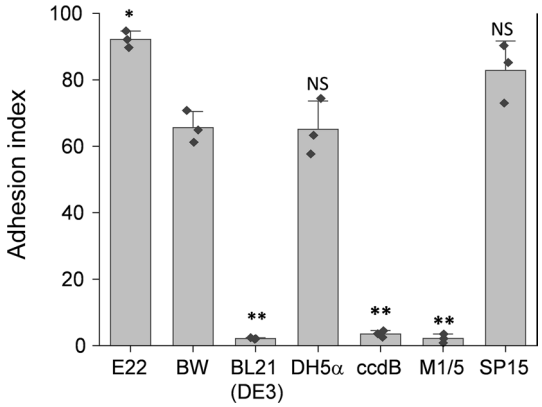

Figure 5. Adhesion to yeast of different strains of *E. coli*. Adhesion capacity of different fluorescent *E. coli* strains was measured *after* the co-incubation of 10^9 cells of *E. coli* strains carrying pet23-IHF-Dendra2 plasmid with 10^8 BY4741 cells. Genotype and origin of the *E. coli* strains are given in Table 1. Kruskal–Wallis ANOVA with Dunn post-test compared to reference *E. coli* BW25113 (BW). *$p<0.05$., **, $p<0.01$; NS: not significant compared to BW25113 strain.

fimbriae[33] and in *fimH* encoding the mannose-binding specific adhesin located at the tip of the fimbriae[34] were co-incubated with yeast BY4741 and adhesion index (A_i) was compared to the reference *E. coli* BW25113 strain. As shown in Fig. 6, A_i was drastically decreased to less than 5% upon deletion of *fimA* or *fimH* genes, supporting a critical role of type 1 fimbriae in the active adhesion of bacteria to yeast. The remaining attachment of *E coli* cells defective in type 1 fimbriae was most likely due to non-specific binding since it could be completely eliminated by an additional 30 min of incubation with the PBS, a condition that was unable to remove the even low amount of *E. coli* BW25113 strain bound to *S. cerevisiae* BY4741 (see Fig. S5 in suppl. data).

Yeast cell wall mannoproteins and other factors contribute to the bacteria adhesion

Yeast cell wall is composed of β-glucans, mannans and chitin at proportion of roughly 55:40:5[35,36]. To investigate the potential implication of these polysaccharides in adhesion, we performed a competition assay in which fluorescent *E. coli* E22 strain was incubated with monosaccharides representing these polysaccharides prior to co-incubation with yeast cells. As shown in Fig. 7A, the adhesion of bacteria to yeast cells was reduced by 90% when 1.0 M of D-mannose or methyl-D-mannose was used in the pre-incubation step, whereas glucose or methyl-glucose that represent β-glucans or N-acetylglucosamine for chitin had no effect. Dose dependent effects of D-mannose and methyl-D-mannose were further tested, showing that methyl-mannose was slightly more potent than mannose to antagonize the adhesion of bacteria to yeast (Fig. 7B). In contrast, adhesion was only partially antagonized when these mannosyl-sugars were added after bacteria and yeast were incubated. This antagonistic effect was at most 30% even in the presence of 1.0 M of methyl mannose (Fig. S6, suppl data),

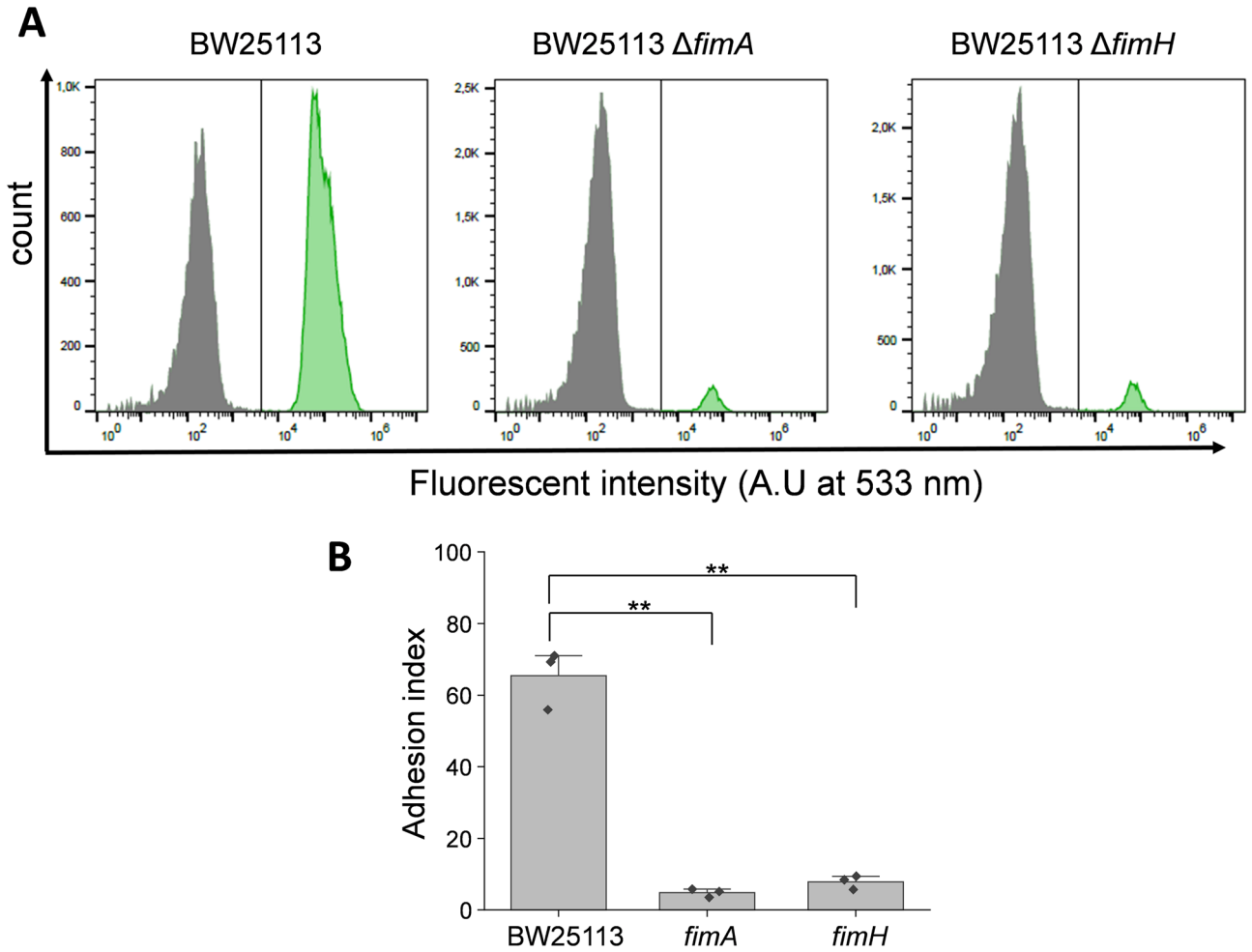

Figure 6. Type 1 fimbriae are essential for adhesion of bacteria to yeast. (**A**) Representative flow cytometer plots of interacted 5×10^8 cells of fluorescent *E. coli* BW25113 or *fimA* and *fimH* mutants with 10^8 of BY4741 yeast cells (**B**) Adhesion index calculated from the results of the three independent interaction experiments. The symbol ** shows significance difference at $p < 0.001$ compared to wild type BW25113 strain.

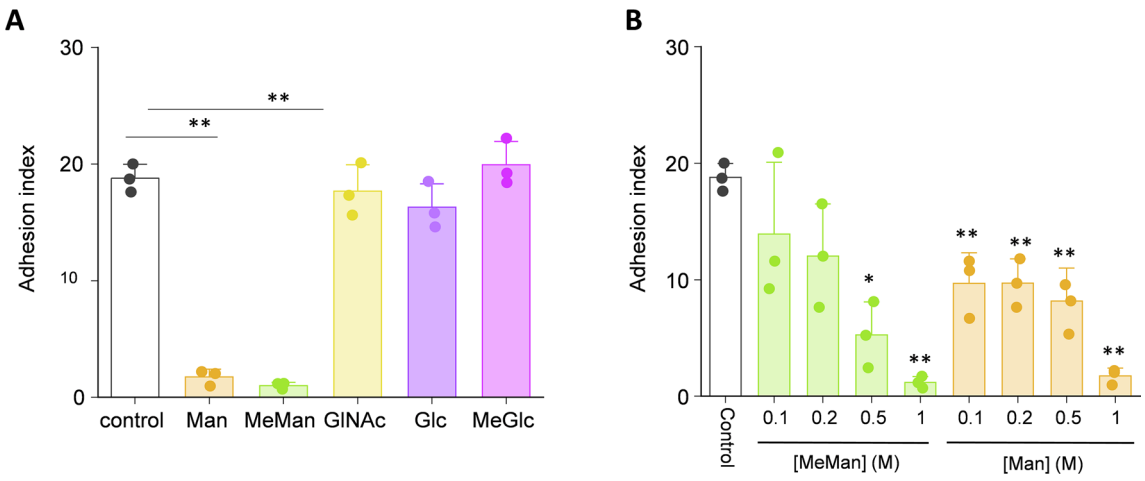

Figure 7. Effects of various sugars on the adhesion of bacteria to yeast. (**A**) 2×10^8 fluorescent *E. coli* E22 preincubated with 1.0 M sugars (GlcNAc, N-acetyl-glucosamine; Man, Mannose; MeMan, Methyl-Mannose; Glc, Glucose; MeGlc, Methyl-Glucose) or with PBS (control) for 30 min before co-incubation with 10^8 yeast BY4741 cell. (**B**) 2×10^8 fluorescent *E. coli* E22 preincubated with increasing concentration of methyl-mannose (Me-Man) or mannose (Man) or with PBS to yeast BY4741 (10^8 cells). The data are the mean of 3 independent biological replicates. **, $P < 0.01$, and *, $P < 0.05$.

and reducing by tenfold the amount of bacteria that were mixed with yeast followed by a washing with 1.0 M mannose solution has almost the same effect (data not shown).

To get further insight on the potential role of cell wall structure in adhesion of bacteria to yeast cells, yeast mutants that are known to have significant alteration in the content of their cell wall polysaccharides were used. Reduction of mannans content in cell wall resulting from the deletion of *MNN1* encoding an alpha-1,2-mannosyltransferase[37] or *OCH1* whose protein is required for polymannose outer chain elongation of *N*-linked oligosaccharides of glycoproteins[38] was accompanied by a not significant decrease in adhesion index as compared to wild type cells (−4.9% and −4.7%, for *mnn1* and *och1* mutant, respectively) (Fig. 8). Same results were obtained with a mutant deleted for *FKS3* which codes for one of the two β-1,3-glucan synthase required for spore wall assembly and which is not reported to alter mannans content[39]. However, a statistically significant increase of adhesion was obtained for the mutant defective in *KRE6* (+15.2%, p = 0.008) which is involved in the biosynthesis of β (1- > 6)-D-glucan and whose deletion was found to reduce proportion of β-glucan as compared to mannan content in the yeast cell wall[36,40]. A trend (+6.7%, p = 0.02) towards increased adhesion was also observed for a mutant defective in *KNR4*, a gene involved in the regulation of cell wall assembly and integrity[41]. Other mutants of the mannan synthesis pathway were tested but did not show any difference from the BY4741 reference strain (data not shown). Overall, these results suggest that it is not simply the presence and quantity of mannans that is important for binding, but also the distribution and/or accessibility of these mannose residues within the polysaccharide structure of the cell wall.

Discussion

The growing interest in the use of probiotics and prebiotics that are mainly formulated from whole yeast and/or from their components for animal and human welfare, notably in the scope of preventing bacterial infections, requires, among other things, a reliable and quantitative method to characterize at the molecular level the interaction of bacteria with these pro-or prebiotics. Here, we report that the flow cytometry perfectly meets this requirement, and compared to previously developed techniques, this method presented the following advantages. Firstly, it enables the analysis of the interaction at the single cell level (yeast singlets) since bacterial and yeast cells can be easily distinguished based on their size and granularity. As a corollary, this method avoids false positive data caused by entrapment of bacteria cells within cell aggregates. In addition, bacteria cells that adhere to yeast cells could be visualized when flow cytometry is coupled to imagery. Another advantage is that this method can be easily adapted to a high-throughput format for screening multiple bacteria-yeast interaction parameters. A slight but not insurmountable drawback of this method is that the bacteria need to be made fluorescent to visualize and quantify the interaction with yeast cells.

A dose-dependent study of bacteria-yeast interaction revealed a hyperbolic curve that has the appearance of a Langmuir isotherm shape. However, as clearly stated by Latour[27] regarding protein adsorption, four basic conditions must be respected to satisfy the Langmuir isotherm model, and one of them is that the adsorption process is dynamically reversible, allowing to calculate equilibrium constant (Keq) and thermodynamic value of the adsorption. However, we found that the interaction of bacteria with yeast cells is rapid and almost non-reversible, as once fluorescent bacteria have been attached to yeast cells, they cannot be removed neither by subjecting them to a large excess of non-fluorescent bacteria, nor under agitation in PBS solution for 24 h at 37 °C. Nevertheless, this kinetic representation allows us to determine a relevant parameter which we have called "α" and that corresponded to the slope of the regression line obtained by plotting $1/A_i$ vs 1/bacteria. This α value can be used as a criterion for distinguishing between candidate bacterial strains or species resulting from large-scale

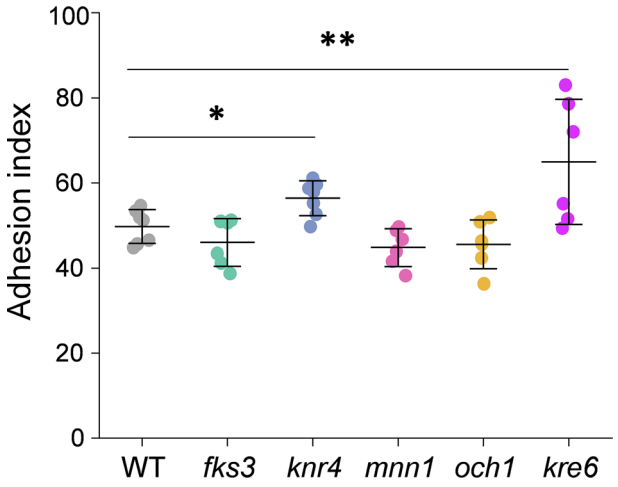

Figure 8. Yeast mutants with altered mannans content in the cell wall had limited effect on the adhesion of *E. coli*. WT corresponded to BY4741 and all the other strains are mutants of this strain deleted for a gene that belong to the cell wall synthesis. Adhesion was measured after the co-incubation of 5×10^8 cells of *E. coli* E22 strain carrying pet23-IHF-Dendra2 with 10^8 yeast cells. The bars are the mean ± SD and individual results of 6 independent biological experiments are reported. *$p < 0.05$., **, $p < 0.01$.

screening for interaction with yeast, bearing in mind also that this value may also depend on the yeast species used for the interaction studies. By coupling flow cytometry to imaging, we were able to measure the number of bacteria attached per yeast and found a maximum of 14 per yeast cell at saturating condition of adhesion. This number of bacteria adhering to the yeast is much lower than what could theoretically be calculated on the basis that the surface of a yeast cell, which is an ovoid object about 5 µm long and 3 µm wide[42] is around 45 μm^2 and that of the bacteria which can be assimilated to a rectangular rod of 2 µm long and 0.5 µm diameter[43] is 1 μm^2. Thus, the maximum would be of the order of 45 bacteria per yeast cell. Additionally, the α value and the number of bacteria adhering to yeast are very likely dependent on bacteria and yeast strains or species.

Although it was already suspected a role of type 1 fimbriae in the interaction of bacteria with yeast as assessed by the agglutination test, showing that the formation of yeast aggregates induced by incubation with bacteria was reduced with bacteria lacking type 1 fimbriae[30–32,44], we here clearly showed that the attachment of bacteria to yeast is fully dependent on the presence of these proteinaceous appendages. Therefore, these results recall those obtained for the adhesion of bacteria to mammalian cells, for which type 1 fimbriae play a determining role[8]. In addition, it was demonstrated that the adhesion of bacteria to mammalian cells is mediated by a catch-bond mechanism of FimH[45], i.e., bonds that become stronger under application of force such as shear stress exerted by the flow of liquids (*e.g.* urine, saliva, mucus). This catch-bond mode to the mannosyl sugars of the glycoproteins present in the membrane of epithelial cells has been explained by conformational states and ligand properties of FimH resulting from its two-domains architecture, namely the N-terminal domain containing the mannose-binding pocket and the C-terminal pilin domain[46,47]. Hence, shear stress or tensile force induces an allosteric switch to a high affinity and strong binding conformation of FimH. It is reported that under these conditions, the attachment of bacteria is permanent or long lived[9,48]. Whether a similar mechanism of adhesion of bacteria to yeast exists remains to be investigated, but the conditions that were set in our work for the interaction between bacteria and yeast cells are very likely in favor of a similar process since pre-incubation was always carried out under shaking, thus under shear-stress conditions.

As type 1 fimbriae were found essential in the interaction of bacteria with yeast cells, and considering that these fimbriae are characterized by a specific mannose-binding pocket at their tips encoded by *fimH*, one could deduce that the interaction of bacteria to yeast cells involve mannosyl-sugars that are very abundant at the cell surface of the yeast wall[12]. The finding that pre-incubation with mannose or methyl-mannose prevented the attachment of bacteria to yeast supported this suggestion. In addition, this FimH-dependent binding could also agree with an avidity phenomenon due to the multivalency of the binding sites (mannosyl-residues) at the yeast cell surface. However, other data in this work suggested that this type 1-fimbriae dependent binding of bacteria to yeast implicated additional factors than the very dense mannosyl units present at the yeast cell surface. Firstly, addition of excess of non-fluorescent bacteria barely competed with previously bound fluorescent bacteria to yeast. Secondly, addition of a 1.0 M concentration mannose solution only caused a partial drop of bacteria bound to yeast. Thirdly, bacteria adhesion to yeast mutants with altered mannans content were not significantly different as compared to the isogenic wild type strain. Although using the questioned co-sedimentation method, Tiago et al.[20] also found no clear correlation between cell wall mannan content and adhesion of *E. coli* or *Salmonella* to yeast cell wall. Ganner et al.[19], using an indirect growth-based assay came to the same conclusion using yeast cell wall with different composition in mannans and β-glucans. Altogether, these results indicate that factors, in addition to mannosyl sugars of the yeast cell wall may participate to the interaction with bacterial cells. This may include the 3D architecture of yeast cell wall, which is the result of complex covalent and non-covalent linkages between β-glucans, chitin and mannoproteins[11,12]. Yeast cell wall structure is very different from the cell surface of epithelial cells, which essentially contains mannosylated proteins. In addition, the yeast cell wall is porous for macromolecules of several kDa[49]. Consequently, type 1 fimbriae could penetrate quite deeply as the wall thickness is of the order of 120–150 nm[49] and thus may anchor bacteria to the yeast wall. Electron microscopy and AFM studies are methods that could be used to address this question.

To conclude, due to its simplicity and reliability, the flow cytometry-based method can be easily adapted for high throughput screening of natural components that can either promote or antagonize adhesion of bacterial to yeast. In addition, this method eventually coupled with imagery could be very useful to pinpoint cellular function implicated in interaction of bacteria and yeast by screening the collection of Keio mutants of *E. coli*[50] and reciprocally the yeast KO collection[51].

Methods

Strains and culture conditions

The yeast BY4741 strain (MATa *his3Δ1 leu2Δ0 met15Δ0 ura3Δ0)* as the reference strain and cell wall mutants *kre6Δ, fks3Δ, gas1Δ, knr4Δ, mnn1Δ and och1Δ* derived from this strain background as described in[51] were obtained from the Yeast Knockout (YKO) collection of Euroscarf (http://www.euroscarf.de/). Yeast strains were cultivated in YPD (2% glucose, 2% Bactopeptone and 1% yeast extract) liquid medium at 30 °C overnight. The list of bacteria strains used in this work with their genotype and origin are provide in Table 1. They were all transformed with the pet3-IHF-Dendra2 plasmid in which the T7 promoter present in the original plasmid (Dagkesamanskaya et al.[52]) was replaced by the strong constitutive IHF promoter from *E.coli*. Culture of bacterial strains were carried out overnight at 37 °C in LB medium with 100 mg/L of ampicillin.

Conditions of co-incubation of bacteria with yeast cells and effects of environmental parameters

After cultivation, cells were harvested by centrifugation, washed once with PBS buffer and resuspended in 1 mL of PBS prior the co-incubation. Bacteria cell number was performed by flow cytometer as they are fluorescent whereas yeast cell number were quantified based on the relationship of 1 unit OD_{600} corresponds to 1.4×10^7

Strain	Phylogenetic group	Genotype	Reference or source
BW25113	A	ΔaraBADAH33 ΔrhaBADLD78 rph-1 Δ(araB–D)567 Δ(rhaD–B)568 ΔlacZ4787(::rrnB-3) hsdR514 rph-1	[50]
BWΔfimA	A	ΔaraBADAH33 ΔrhaBADLD78 rph-1 Δ(araB–D)567 Δ(rhaD–B)568 ΔlacZ4787(::rrnB-3) hsdR514 rph-1 ΔfimA	[50]
BWΔfimH	A	ΔaraBADAH33 ΔrhaBADLD78 rph-1 Δ(araB–D)567 Δ(rhaD–B)568 ΔlacZ4787(::rrnB-3) hsdR514 rph-1 ΔfimH	[50]
BL21(DE3)	A	F⁻ompT hsdSB (rB–, mB–) gal dcm (DE3)	New England BioLabs
DH5α	A	F⁻ φ80*lac*ZΔM15 Δ(*lac*ZYA-*arg*F)U169 *rec*A1 *end*A1 *hsd*R17(r_K^-, m_K^+) *pho*A *sup*E44 λ⁻*thi*-1 *gyr*A96 *rel*A1	New England BioLabs
*ccd*B Survival™	A	F ⁻*mcr*A Δ(*mrr-hsd*RMS-*mcr*BC) φ80*lac*ZΔM15 Δ*lac*X74 *rec*A1 *ara*Δ139 Δ(*ara-leu*)7697 *gal*U *gal*K *rps*L(Str^R) *end*A1 *nup*G *fhu*A::*IS2*	Invitrogen™
E22	B1	REPEC O103:K-H2, rhamnose-negative strain	[53]
SP15	B2	not known	[54]
M1/5	B2	Not known	[55]

Table 1. List of strains with genotype and reference used in this work.

cells/ml. For the cell wall mutants in general and in particular *gas1Δ*, known to show strong cell–cell aggregation, a 10 s. sonication in PBS buffer was performed before mixing with fluorescent *E. coli*. Unless otherwise stated, the co-incubation experiments were carried out by mixing of 1 ml of 10^8 yeast cells with 0.5 ml of 2×10^9 *E. coli* cells in PBS. Mixture was incubated with agitation in 2 mL Eppendorf tube at 37 °C for 90 min. This mix was then spun down for 5 s using low speed centrifuge (1000g at room temperature) to allow yeast cells to sediment while most of the free *E. coli* cells remained in the supernatant. After removal of the supernatant, the pellet was re-suspended in 1 mL of PBS, centrifuged (1000g at room temperature) and this operation was repeated once more time before flow cytometry analysis.

Flow cytometry and imaging flow cytometry analyses

All samples were measured on a BD Accuri™ C6 Plus flow cytometer (BD Bioscience) equipped with a laser exciting at a wavelength of 488 nm. Before each experiment, the calibration of the flow cytometer was assessed with calibration beads (BDTM CS&T RUO Beads; BD Biosciences). Acquisition parameters were set at a flow rate of 14 µl/min and 10 µm core size with a threshold at 10,000 on SSC-Height signal. A first gate was applied to select the population corresponding to yeast cells which was based on the dot plot of the forward scatter channel (FSC-Area) versus side scatter channel (SSC-Area) that excluded free bacteria. In addition, based on the FSC-Area *vs* FSC-Height dot plot, single yeast (singlets) cells with similar cell size and granularity were selected by applying a second gate (Fig. S1). The Dendra2 green fluorescence emissions of the bacteria were analyzed with the FL1 channel (533/30 nm). Finally, the adhesion index (A_i) was computed as the amount of yeast singlets with bound green, fluorescent bacteria (FL1 channel) divided by the total number of yeast singlets × 100. Data acquisition was set at 100,000 events per sample and after applying the two gates at least 70,000 events of single yeast cells were analyzed per sample. Data were analyzed with FlowJo v10 software (BD Bioscience) and same gates were applied to all the data, to ensure that it included the entire population especially in the case of morphological variations between strains. No variations in cell population between yeast strains used in this study were seen, except for the strain *gas1Δ*.

Imaging flow cytometry of mix of bacteria (5×10^9 cell/ml) and yeast (10^8 cell/ml) initially preincubated for 90 min at 37 °C was acquired on the ImageStreamX Mark II (Amnis-EMD Millipore). Yeasts were selected on the basis of their size on dot plot Area and Aspect ratio on the brightfield. For each experiment, 1000 yeast per sample were acquired (ensuring a sufficient number of events remaining for statistically robust analysis) at 60X magnification. Image analysis was completed using image-based algorithms in the ImageStream Data Exploration and Analysis Software (IDEAS_6.2.64.0, EMD Millipore). The number of fluorescent bacteria puncta per yeast was assessed with the feature "Spot Counting". A mask based on GFP staining was employed (SpotCount_Peak [M02, Ch02, Bright, 18.95]_4) to visualize bacteria. The same mask and feature were automatically applied for each condition.

Microscopy analysis

Qualitative interaction between yeast and fluorescent bacteria was evaluated under optical microscope using a Leica DM4000B microscope with Leica EL6000 light source at wavelength of 490 nm for excitation and 530 nm for emission. Pictures were taken using a LEICA DFC300FX camera.

Langmuir isotherm model

Isotherm data were obtained by co-incubation experiments performed with BY4741 strain at a fixed concentration (1×10^8 cells/mL) and various initial concentration of bacteria strains E22 and BW25113 (from 5×10^6 to 10^{10} cells/mL). After incubation for 1.5h at 37 °C in PBS pH7, suspensions were washed as described above and analyzed by flow cytometry.

The adhesion of bacteria B to yeast Y can be written as

$$B + Y \leftrightarrow \mathrm{BY}_{\mathrm{ads}}$$

Giving the following equation:

$$BY_{ads} = BY_{adsmax} \times \frac{a[Bact]}{1 + a[Bact]} \quad (1)$$

with BY_{ads} (cells. mL^{-1}) is the amount of bacteria that bind to yeast and is obtained by the fluorescence measurement of bacteria. BY_{adsmax} is the max of adhesion of bacteria to yeast cells, [Bact] is the initial concentration of bacteria added to a fixed concentration of yeast cells and a is a "constant" value that specific to the bacteria strain and that approximate its dsorption capacity. It is expressed as number of cells per mL. In this study, the BY_{ads} is assimilated to A_i and therefore, the equation of bacteria—yeast interaction can be rewritten as

$$A_i = A_{imax} \times \frac{a[Bact]}{1 + a[Bact]} \quad (2)$$

$$\frac{1}{A_i} = \frac{1}{A_{imax} \times a} \times \frac{1}{[Bact]} + \frac{1}{A_{imax}} \quad (3)$$

$$\text{The slope } \alpha = \frac{1}{a \times A_{imax}} \quad (4)$$

and thus $\alpha \sim 1/a$ since $Ai_{max} = 100$ for all bacteria

Experimental data were fitted by Eq. (4) and the correlation coefficient (r^2) was used to measure the best fitting of the isotherm to the experimental data.

Statistical analysis

All assays were carried out at least 3 times with n independent biological samples (n being specified in each figure). Statistical analysis was performed using OriginPro (version 9.7.0.185) using nonparametric test Kruskal–Wallis ANOVA with Dunn post-hoc analysis. Significant values were denoted by asterisks on the figures as **: $P < 0.01$, and *: $P < 0.05$. NS, not significant.

Data availability

Data is provided within the manuscript or supplementary information files.

Received: 2 May 2024; Accepted: 3 September 2024
Published online: 09 September 2024

References

1. Pontier-Bres, R. *et al.* Saccharomyces boulardii modifies Salmonella typhimurium traffic and host immune responses along the intestinal tract. *PLoS ONE* **9**, e103069. https://doi.org/10.1371/journal.pone.0103069 (2014).
2. Mourão, J. L. *et al.* Effect of mannan oligosaccharides on the performance, intestinal morphology and cecal fermentation of fattening rabbits. *Anim. Feed Sci. Technol.* **126**, 107–120. https://doi.org/10.1016/j.anifeedsci.2005.06.009 (2006).
3. Terré, M., Calvo, M. A., Adelantado, C., Kocher, A. & Bach, A. Effects of mannan oligosaccharides on performance and microorganism fecal counts of calves following an enhanced-growth feeding program. *Anim. Feed Sci. Technol.* **137**, 115–125. https://doi.org/10.1016/j.anifeedsci.2006.11.009 (2007).
4. Spring, P., Wenk, C., Dawson, K. A. & Newman, K. E. The effects of dietary mannaoligosaccharides on cecal parameters and the concentrations of enteric bacteria in the ceca of salmonella-challenged broiler chicks. *Poult. Sci.* **79**, 205–211. https://doi.org/10.1093/ps/79.2.205 (2000).
5. Posadas, G. A. *et al.* Yeast pro- and paraprobiotics have the capability to bind pathogenic bacteria associated with animal disease. *Transl. Anim. Sci.* **1**, 60–68. https://doi.org/10.2527/tas2016.0007 (2017).
6. Sharon, N. & Ofek, I. Safe as mother's milk: carbohydrates as future anti-adhesion drugs for bacterial diseases. *Glycoconj. J.* **17**, 659–664. https://doi.org/10.1023/a:1011091029973 (2000).
7. Snellings, N. J., Tall, B. D. & Venkatesan, M. M. Characterization of Shigella type 1 fimbriae: expression, FimA sequence, and phase variation. *Infect. Immun.* **65**, 2462–2467. https://doi.org/10.1128/iai.65.6.2462-2467.1997 (1997).
8. Knight, S. D. & Bouckaert, J. Structure, function, and assembly of type 1 fimbriae. *Top. Curr. Chem.* **288**, 67–107. https://doi.org/10.1007/128_2008_13 (2009).
9. Feenstra, T. *et al.* Adhesion of Escherichia coli under flow conditions reveals potential novel effects of FimH mutations. *Eur. J. Clin. Microbiol. Infect. Dis.* **36**, 467–478. https://doi.org/10.1007/s10096-016-2820-8 (2017).
10. McLay, R. B. *et al.* Level of fimbriation alters the adhesion of *Escherichia coli* bacteria to interfaces. *Langmuir* **34**, 1133–1142. https://doi.org/10.1021/acs.langmuir.7b02447 (2018).
11. Klis, F. M., Mol, P., Hellingwerf, K. & Brul, S. Dynamics of cell wall structure in Saccharomyces cerevisiae. *FEMS Microbiol. Rev.* **26**, 239–256 (2002).
12. Orlean, P. Architecture and biosynthesis of the Saccharomyces cerevisiae cell wall. *Genetics* **192**, 775–818 (2012).
13. Gow, N. A. R. & Lenardon, M. D. Architecture of the dynamic fungal cell wall. *Nat. Rev. Microbiol.* **21**, 248–259. https://doi.org/10.1038/s41579-022-00796-9 (2023).
14. Xu, X., Qiao, Y., Peng, Q., Gao, L. & Shi, B. Inhibitory effects of YCW and MOS from *Saccharomyces cerevisiae* on *Escherichia coli* and Salmonella pullorum adhesion to Caco-2 cells. *Front. Biol.* **12**, 370–375. https://doi.org/10.1007/s11515-017-1464-0 (2017).
15. Sauvaitre, T. *et al.* Lentils and yeast fibers: A new strategy to mitigate enterotoxigenic *Escherichia coli* (ETEC) strain H10407 virulence?. *Nutrients* https://doi.org/10.3390/nu14102146 (2022).
16. Ageorges, V. *et al.* Genome-wide analysis of antigen 43 (Ag43) variants: New insights in their diversity, distribution and prevalence in bacteria. *Int. J. Mol. Sci.* https://doi.org/10.3390/ijms24065500 (2023).
17. Mammarappallil, J. G. & Elsinghorst, E. A. Epithelial cell adherence mediated by the enterotoxigenic *Escherichia coli* Tia protein. *Infect. Immun.* **68**, 6595–6601. https://doi.org/10.1128/iai.68.12.6595-6601.2000 (2000).
18. Ganner, A. & Schatzmayr, G. Capability of yeast derivatives to adhere enteropathogenic bacteria and to modulate cells of the innate immune system. *Appl. Microbiol. Biotechnol* **95**, 289–297. https://doi.org/10.1007/s00253-012-4140-y (2012).

19. Ganner, A., Stoiber, C., Uhlik, J. T., Dohnal, I. & Schatzmayr, G. Quantitative evaluation of *E. coli* F4 and *Salmonella Typhimurium* binding capacity of yeast derivatives. *AMB Express* **3**, 62. https://doi.org/10.1186/2191-0855-3-62 (2013).
20. Tiago, F. C. P. *et al.* Adhesion to the yeast cell surface as a mechanism for trapping pathogenic bacteria by Saccharomyces probiotics. *J. Med. Microbiol.* **61**, 1194–1207. https://doi.org/10.1099/jmm.0.042283-0 (2012).
21. Martyniak, A., Medyńska-Przęczek, A., Wędrychowicz, A., Skoczeń, S. & Tomasik, P. J. Prebiotics, probiotics, synbiotics, paraprobiotics and postbiotic compounds in IBD. *Biomolecules* https://doi.org/10.3390/biom11121903 (2021).
22. Mirelman, D., Altmann, G. & Eshdat, Y. Screening of bacterial isolates for mannose-specific lectin activity by agglutination of yeasts. *J. Clin. Microbiol.* **11**, 328–331. https://doi.org/10.1128/jcm.11.4.328-331.1980 (1980).
23. Pérez-Sotelo, L. S. *et al.* In vitro evaluation of the binding capacity of Saccharomyces cerevisiae Sc47 to adhere to the wall of Salmonella spp. *Rev. Latinoam. Microbiol.* **47**, 70–75 (2005).
24. Becker, P. M., Galletti, S., Roubos-van den Hil, P. J. & van Wikselaar, P. G. Validation of growth as measurand for bacterial adhesion to food and feed ingredients. *J. Appl. Microbiol.* **103**, 2686–2696. https://doi.org/10.1111/j.1365-2672.2007.03524.x (2007).
25. Millsap, K. W., van der Mei, H. C., Bos, R. & Busscher, H. J. Adhesive interactions between medically important yeasts and bacteria. *FEMS Microbiol. Rev.* **21**, 321–336. https://doi.org/10.1111/j.1574-6976.1998.tb00356.x (1998).
26. Popolo, L. & Vai, M. The Gas1 glycoprotein, a putative wall polymer cross-linker. *Biochim. Biophys. Acta* **1426**, 385–400 (1999).
27. Latour, R. A. The Langmuir isotherm: a commonly applied but misleading approach for the analysis of protein adsorption behavior. *J. Biomed. Mater. Res. A* **103**, 949–958. https://doi.org/10.1002/jbm.a.35235 (2015).
28. Han, M.-J. Exploring the proteomic characteristics of the Escherichia coli B and K-12 strains in different cellular compartments. *J. Biosci. Bioeng.* **122**, 1–9. https://doi.org/10.1016/j.jbiosc.2015.12.005 (2016).
29. Thoma, J. *et al.* Protein-enriched outer membrane vesicles as a native platform for outer membrane protein studies. *Commun. Biol.* **1**, 23. https://doi.org/10.1038/s42003-018-0027-5 (2018).
30. Schembri, M. A., Sokurenko, E. V. & Klemm, P. Functional flexibility of the FimH adhesin: Insights from a random mutant library. *Infect. Immun.* **68**, 2638–2646. https://doi.org/10.1128/iai.68.5.2638-2646.2000 (2000).
31. Eshdat, Y., Speth, V. & Jann, K. Participation of pili and cell wall adhesion in the yeast agglutination activity of *Escherichia coli*. *Infect. Immun.* **34**, 980–986. https://doi.org/10.1128/iai.34.3.980-986.1981 (1981).
32. Korhonen, T. K., Leffler, H. & Svanborg Eden, C. Binding specificity of piliated strains of *Escherichia coli* and *Salmonella typhimurium* to epithelial cells, *Saccharomyces cerevisiae* cells, and erythrocytes. *Infect. Immun.* **32**, 796–804. https://doi.org/10.1128/iai.32.2.796-804.1981 (1981).
33. Russell, P. W. & Orndorff, P. E. Lesions in two *Escherichia coli* type 1 pilus genes alter pilus number and length without affecting receptor binding. *J. Bacteriol.* **174**, 5923–5935. https://doi.org/10.1128/jb.174.18.5923-5935.1992 (1992).
34. Jones, C. H. *et al.* FimH adhesin of type 1 pili is assembled into a fibrillar tip structure in the Enterobacteriaceae. *Proc. Natl. Acad. Sci. USA* **92**, 2081–2085. https://doi.org/10.1073/pnas.92.6.2081 (1995).
35. Uscanga, B. Influence de paramètres de croissance et des conditions de mise en oeuvre sur la compoistion et l'architecture de la paroi cellulaire de la levure. Ph D Thesis, no from the "Institut National Des Sciences Appliquées", Toulouse, 174 (2003).
36. Schiavone, M. *et al.* A combined chemical and enzymatic method to determine quantitatively the polysaccharide components in the cell wall of yeasts. *FEMS Yeast Res.* **14**, 933–947. https://doi.org/10.1111/1567-1364.12182 (2014).
37. Lussier, M., Sdicu, A. M., Ketela, T. & Bussey, H. Localization and targeting of the *Saccharomyces cerevisiae* Kre2p/Mnt1p alpha 1,2-mannosyltransferase to a medial-Golgi compartment. *J. Cell Biol.* **131**, 913–927 (1995).
38. Nakayama, K., Nagasu, T., Shimma, Y., Kuromitsu, J. & Jigami, Y. *OCH1* encodes a novel membrane bound mannosyltransferase: Outer chain elongation of asparagine-linked oligosaccharides. *EMBO J.* **11**, 2511–2519 (1992).
39. Ishihara, S. *et al.* Homologous subunits of 1,3-beta-glucan synthase are important for spore wall assembly in *Saccharomyces cerevisiae*. *Eukaryot. Cell* **6**, 143–156. https://doi.org/10.1128/ec.00200-06 (2007).
40. Dallies, N., Francois, J. & Paquet, V. A new method for quantitative determination of polysaccharides in the yeast cell wall. Application to the cell wall defective mutants of *Saccharomyces cerevisiae*. *Yeast* **14**, 1297–1306 (1998).
41. Martin-Yken, H., Francois, J. M. & Zerbib, D. Knr4: A disordered hub protein at the heart of fungal cell wall signalling. *Cell Microbiol.* **18**, 1217–1227. https://doi.org/10.1111/cmi.12618 (2016).
42. Jorgensen, P., Nishikawa, J. L., Breitkreutz, B. J. & Tyers, M. Systematic identification of pathways that couple cell growth and division in yeast. *Science* **297**, 395–400 (2002).
43. Osiro, D., Filho, R. B., Assis, O. B., Jorge, L. A. & Colnago, L. A. Measuring bacterial cells size with AFM. *Braz. J. Microbiol.* **43**, 341–347. https://doi.org/10.1590/s1517-83822012000100040 (2012).
44. Wu, K.-H., Wang, K.-C., Lee, L.-W., Huang, Y.-N. & Yeh, K.-S. A constitutively mannose-sensitive agglutinating *Salmonella enterica* subsp. enterica *Serovar Typhimurium* strain, carrying a transposon in the fimbrial usher gene stbC, exhibits multidrug resistance and flagellated phenotypes. *Sci. World J.* **2012**, 280264. https://doi.org/10.1100/2012/280264 (2012).
45. Thomas, W. Catch bonds in adhesion. *Annu. Rev. Biomed. Eng.* **10**, 39–57. https://doi.org/10.1146/annurev.bioeng.10.061807.160427 (2008).
46. Forero, M., Yakovenko, O., Sokurenko, E. V., Thomas, W. E. & Vogel, V. Uncoiling mechanics of *Escherichia coli* type I fimbriae are optimized for catch bonds. *PLoS Biol.* **4**, e298. https://doi.org/10.1371/journal.pbio.0040298 (2006).
47. Yakovenko, O. *et al.* FimH forms catch bonds that are enhanced by mechanical force due to allosteric regulation. *J. Biol. Chem.* **283**, 11596–11605. https://doi.org/10.1074/jbc.M707815200 (2008).
48. Thomas, W. E. *et al.* Recombinant FimH adhesin demonstrates how the allosteric catch bond mechanism can support fast and strong bacterial attachment in the absence of shear. *J. Mol. Biol.* **434**, 167681. https://doi.org/10.1016/j.jmb.2022.167681 (2022).
49. Francois, J. M. Cell surface interference with plasma membrane and transport processes in yeasts. *Adv. Exp. Med. Biol* **892**, 11–31. https://doi.org/10.1007/978-3-319-25304-6_2 (2016).
50. Baba, T. *et al.* Construction of Escherichia coli K-12 in-frame, single-gene knockout mutants: The Keio collection. *Mol. Syst. Biol.* https://doi.org/10.1038/msb4100050 (2006).
51. Brachmann, C. B. *et al.* Designer deletion strains derived from Saccharomyces cerevisiae S288C: A useful set of strains and plasmids for PCR-mediated gene disruption and other applications. *Yeast* **14**, 115–132. https://doi.org/10.1002/(sici)1097-0061(19980130)14:2%3c115::Aid-yea204%3e3.0.Co;2-2 (1998).
52. Dagkesamanskaya, A. *et al.* Use of photoswitchable fluorescent proteins for droplet-based microfluidic screening. *J Microbiol Methods.* **147**, 59–65. https://doi.org/10.1016/j.mimet.2018.03.001 (2018).
53. Marches, O. *et al.* Role of tir and intimin in the virulence of rabbit enteropathogenic *Escherichia coli* serotype O103:H_2. *Infect. Immun.* **68**, 2171–2182. https://doi.org/10.1128/IAI.68.4.2171-2182.2000 (2000).
54. Johnson, J. R., Johnston, B., Kuskowski, M. A., Nougayrede, J. P. & Oswald, E. Molecular epidemiology and phylogenetic distribution of the *Escherichia coli* pks genomic island. *J. Clin. Microbiol.* **46**, 3906–3911. https://doi.org/10.1128/jcm.00949-08 (2008).
55. Martin, P. *et al.* Interplay between Siderophores and Colibactin Genotoxin biosynthetic pathways in *Escherichia coli*. *PLOS Pathog.* **9**, e1003437. https://doi.org/10.1371/journal.ppat.1003437 (2013).

Acknowledgements

We are grateful to Dr. Jean-Philippe Nougayrède from IRSD, Toulouse, France for the kind gift of clinical isolates of *E. coli*.

Author contributions

M.S., A.D. and J.M.F. conceived the study. M.S., A.D. and P-J.V. Performed the experiments with M.D. Providing guidance with the use of flow cytometer. A.D and V. D-E. Performed imaging flow cytometry experiments. J.M.F., M.S and A.D. Wrote the paper and all authors read and approved the final version.

Funding

This work was supported in part by industrial grants (project Lallwall, No. SAIC2016/048 & SAIC/2018/010) to J.M.F.

Competing interests

The authors declare no competing interests.

Additional information

Supplementary Information The online version contains supplementary material available at https://doi.org/10.1038/s41598-024-72030-w.

Correspondence and requests for materials should be addressed to J.M.F.

Reprints and permissions information is available at www.nature.com/reprints.

Publisher's note Springer Nature remains neutral with regard to jurisdictional claims in published maps and institutional affiliations.